Water Soluble Polymer-Surfactant Complexes-Stabilized Pd(0) Nanocatalysts: Characterization and Structure-Activity Relationships in Biphasic Hydrogenation of Alkenes and α,β-Unsaturated Ketones

Brunno L. Albuquerque [a,b], Audrey Denicourt-Nowicki [b], Cristelle Mériadec [c], Josiel B. Domingos* [a], and Alain Roucoux* [b]

a LaCBio - Laboratory of Biomimetic Catalysis, Chemistry Department, Universidade Federal de Santa Catarina, Campus Trindade, 88040-900, Florianópolis – SC, Brazil

b École Nationale Supérieure de Chimie de Rennes, CNRS, UMR 6226, 11 Allée de Beaulieu, CS 50837, 35 708 Rennes Cedex 7, France

c Institut de Physique de Rennes UMR UR1-CNRS 6251, Université de Rennes 1, Campus de Beaulieu, CS74205, 35042 Rennes Cedex, France

(*) Corresponding authors: E-mail addresses: alain.roucoux@ensc-rennes.fr (A. R.), josiel.domingos@ufsc.br (J.B.D).

Abstract

A suitable approach to stabilize palladium nanoparticles in water as a green reaction medium for catalytic hydrogenation reactions is described. Supramolecular self-assemblies, obtained through the mixture of modified polyethyleneimines as amphiphilic polymers and water-soluble ammonium salts as surfactants, were used as efficient protective agents in the synthesis of Pd(0) nanospecies. The size and dispersion of the nanoparticles prepared with these original self-assemblies were characterized by TEM, SAXS and DLS techniques. The performances of the catalysts according to the polymer-surfactant mixtures were investigated in the hydrogenation of alkenes and *α,β*-unsaturated ketones in pure biphasic water/substrate medium, under mild conditions (room temperature and 1 bar H_2). The

nanocatalysts showed efficient catalytic activities and selectivity towards C=C bonds. From investigations, the polymer-surfactant complexes act as cooperative protective agents and a pertinent structure-activity relationship was proposed based on the zeta-potential values and the catalytic activity of the resulting colloids.

Keywords

Palladium; Hydrogenation; Polymer; Surfactant; Supramolecular self-assemblies; Nanoparticles; Water

Introduction

Playing a central role in nanoscience and nanotechnology [1-4], catalysis has driven much research efforts in the past decades in the design of nanostructures with well-controlled size, shape and morphology [5-9]. However, the development of well-stable, highly active and selective nanocatalysts still remains a challenge and a growing subject at academic and industry levels.

For more than a century, palladium has been used as a reference catalyst for alkene hydrogenation [10]. Over the past years, new routes to employ this efficient catalyst have been developed [11]. Among them, nanometer-sized palladium particles have proven to be pertinent candidates for synthetic transformations, owing to their outstanding surface properties, and dispersed or supported palladium nanoparticles (Pd^0NPs) have been widely studied for diverse catalytic applications [12-15].

Nowadays, in the drive towards an eco-responsible chemistry, the use of greener media, thus limiting volatile organic solvents, is strongly encouraged. For that purpose, water has appeared as a relevant reaction medium [16], being available, environmentally benign [17-19] and leading to easy work-up [20]. Therefore, the development of colloidal Pd^0NPs stabilized in aqueous solution proved to be a relevant approach towards green chemical processes [21].

Besides their protective role to produce stable and size-controlled nanoparticles, the capping agents could also be chosen to transfer their physico-chemical properties to the nanocatalysts [22], thus influencing the substrate's solubility or the selectivity during the catalytic process [23]. For instance, Neumann and coworkers [24] have reported the chemoselective stereocontrolled hydrogenation of alkenes by Pd^0NPs stabilized with alkylated-polyethyleneimine (Alk-PEI). They have shown that in combination with the steric hindrance of the substrates, the structure of the Alk-PEI protective agents influences the reaction rate [24]. Similarly, Crooks and coworkers studied the hydrogenation of allylic alcohols by Pd nanoparticles in water/methanol 4:1 mixtures. From their results, higher generations of dendrimers can act as a nanofilter in which steric demanding substrates were reacted in slower rates [25].

Polymer-surfactant self-assemblies in liquid phase have been studied for over more than half a century [26]. However, the use of such potential supramolecular organizations as capping agents of metal nanoparticles still remains poorly investigated. Based on their structural characteristics, amphiphilic polymers and surfactants self-assemblies, such as modified–PEI, could produce thermodynamically stable catalysts, and potentially offer novel and original physico-chemical properties [27-29]. The driving force for the self-assembly of amphiphilic compounds relies on hydrophobic effects between the apolar counterparts of the molecules [30]. These self-assembled supramolecular complexes thus provide potential candidates for the stabilization of catalytically active Pd^0NPs, due to the modulation of the physico-chemical properties upon the variation of their components.

In the present work, we report the use of supramolecular self-assemblies, composed of an ammonium surfactant, namely *N,N*-dimethyl-*N*-hexadecyl-*N*-(2-hydroxyethyl)ammonium chloride salt (HEA16Cl) [31], and a *N*-dodecylated PEI, as protective agents of Pd^0 nanospecies. These nanocatalysts have been evaluated in the hydrogenation reaction of alkenes and various *α,β*-unsaturated ketones (enones) as functionalized alkenes, in terms of catalytic activity and selectivity under very mild reaction and biphasic water/substrate conditions (Figure 1). For a better understanding in their

supramolecular behaviours and correlation with catalytic investigations, these novel self-assemblies have been fully characterized by scattering techniques (light and X-ray based), Transmission Electron Microscopy (TEM) and zeta potential measurements to determine the size of the colloids, both the metallic core and the protective layer.

- Figure 1 -

1. Experimental

1.1 Materials and Methods.

Randomly branched PEI 800 Da (Aldrich, composed of 25/50/25 % of primary/secondary/tertiary amines), disodium tetrachloropalladate (Strem Chemicals), sodium borohydride (Acros Organics), substrates and product standards were purchased from commercial sources and used as received without any further purification. All solvents were spectroscopic grade and ultrapure water was used in all systems. The surfactant HEA16Cl was prepared according to previously described method [31].

1.2 Synthesis of M6PEI.

In a round-bottomed flask, PEI (800 Da, 5.5 g, 0.180 mol in monomer units) was dissolved in MeOH (55 mL) under magnetic stirring. Dodecyl aldehyde (5.90 g, 0.032 mol) in THF solution (10 mL) was added and the resulting mixture was stirred at room temperature for 24h. Then, $NaBH_4$ (1.34 g, 0.0352 mol) was introduced over the reaction mixture and stirred for more 12h to ensure complete reduction of the imines formed during the reaction. After that period, the reaction mixture was poured into a dialysis membrane (Spectrapor, 1000 g mol^{-1} cut off) and dialyzed for 5 days over distilled water (3 L) with solvent change every 12h. The degree of alkylation was determined by ^1H NMR by the integration of alkyl chains over the alkylic protons in PEI backbone. The average molecular weight of 1800 g mol^{-1} of M6PEI was determined by ^1H NMR. ^1H NMR (200 MHz, $CDCl_3$): δ = 0.81 (m, 18H), 1.23 (m, 120H), 2.5-2.75 (m, 80H).

1.3 *cmc* and *cac* determinations of M6PEI and HEA16Cl self-assemblies

The determination of critical micelle concentration (*cmc*) and critical aggregation concentration (*cac*), based on the MW of M6PEI monomer units (43 g mol^{-1}) and HEA16Cl concentrations, respectively, were made in a Hitachi F-4500 fluorescence spectrophotometer using standard fluorescence quartz cuvette thermostated at 25.0 ± 0.1 ºC equipped with a magnetic stirrer. The pyrene emission spectrum was obtained using an excitation at 336 nm with the excitation/emission slits set at 2.5 nm.

An aqueous solution of pyrene (1.0 µmol L^{-1}) prepared by dissolution of an ethanolic pyrene solution (1.0 mmol L^{-1}) in water was used to prepare the M6PEI, HEA16Cl and M6PEI-HEA16Cl solutions. The intensities values of the first (372.8 nm, I_1) and the third (384.0 nm, I_3) pyrene emission peaks were used for the I_1/I_3 ratio [27-29].

1.4 Synthesis of Pd^0NPs.

In a typical synthesis, a freshly prepared aqueous solution of 10 mL of $NaBH_4$ (0.3 mmol, 11.35 mg) was rapidly added under vigorous magnetic stirring to a 40 mL aqueous solution of Na_2PdCl_4 (0.075 mmol, 22.10 mg) and stabilizer (surfactant, polymer or mixture) (0.375 mmol). The formation of the Pd^0NPs is visually characterized by a colour change from yellow to dark brown.

1.5 Characterization of Pd^0NP colloids.

The Pd^0NPs@stabilizer suspensions were characterized by TEM, scattering techniques and zeta potential values. For the TEM analysis, four drops of the aqueous colloidal NPs were deposited on a 400-square mesh copper grid with carbon film and dried naturally. The micrographs were acquired using a JEOL JEM-1011 electron microscope operating at 100 kV. At least 140 particles were considered to plot a histogram of the NP size distribution, and the average particle size was obtained by a Gaussian fit of the size distribution. The dynamic light scattering (DLS) experiments and zeta potential were carried out using a DelsaNano C instrument (Beckmann Coulter). The aqueous suspensions of Pd^0NP were analysed at 25 ºC, after the temperature equilibration, about 10 min after the cell

was placed in the DLS apparatus. SAXS experiments were performed on the SAXS1 beam line of the Brazilian Synchrotron Light Laboratory (LNLS – Campinas, SP, Brazil) and at the Institut de Physique in Université de Rennes1, France. The system configuration for the experiments carried out in LNLS (Brazil) was made as in our recent publications [32-34]. The solutions were loaded into a temperature-controlled vacuum flow-through cell composed of two mica windows separated by 1 mm, normal to the beam [35]. For the experiments carried out on the SAXS1 beam line, the collimated beam (λ = 1.55 Å) crossed the sample through an evacuated flight tube and was scattered to a Pilatus 300K 2D detector (Dectris) and a 2D CCDmarCCD 165 detector, respectively. The incident beam was detected at two different sample-to-detector distances on the SAXS1 beam line, 500 mm (silver behenate was used for sample-to-detector distance calibration), to achieve the scattering vector range q (from 0.1 to 5 nm^{-1}). The experiments carried out in the bench-top configuration, X-ray patterns were collected with a Pilatus 300k (Dektris, Grenoble, France), mounted on a microsource X-ray generator GeniX 3D (Xenocs, Sassenage, France) operating at 30 watts. The monochromatic CuKα radiation is λ = 1.541 Å. The diffraction patterns were therefore recorded for reciprocal spacing $q = 4\pi*\sin\theta/\lambda$ in a range of repetitive distances from 0.15 nm^{-1} (4180 nm) and 7.7 nm^{-1} (80 nm). The samples were loaded in quartz capillary tubes (ø = 1.1 mm) and the tubes placed in a homemade sample holder. For both experimental set ups the 2D images were found to be isotropic and they were normalized using the FIT2D software developed by A. Hammersley [36]. Also, the resulting I (q) vs. q scattering curves were corrected by subtraction of the scattering from the pure solvent and then placed on an absolute scale using water as the standard. The log (q) vs. log q^{-1} scattering profile of the Pd^0NPs could be fitted using the Beaucage Power Law [37] and Core-Shell models [38]. The fitting procedures and other analysis were performed using the SASfit software developed by J. Kohlbrecher and available free of charge [39], which makes use of the least squares fitting approach to minimize the chi squared (χ^2) parameter.

1.6 Catalytic activity studies.

In a Schlenk tube, 10 mL of the colloidal Pd^0NPs (0.015 mmol) and the substrate (1.5 mmol) were introduced. The mixture is strongly stirred with a magnetic bar, covered with a septum and degasified over vacuum. After the bubble evolution ceases, a balloon filled with H_2 is attached in the septum and the degasification procedure is repeated at least 2 times. For kinetic experiments, one aliquot of the reaction mixture (± 1.0 mL) is removed at a desired time with a syringe and the organic compounds are extracted with diethyl ether for GC analysis (Carrier gas He, Isobaric at 60 kPa, Column CP-Chirasil-Dex-CB – 30 m x 0.25 mm x 0.25 µm, oven temperature varies with substrate, injector at 250 ºC and FID Detector at 250 ºC).

2. Results and Discussion

2.1 Synthesis and stability of Pd^0NPs.

The Pd^0NPs catalytic systems (Figure 1) were prepared in the presence of various protective agents, such as HEA16Cl surfactant, the N-dodecylated PEI (M6PEI) or HEA16Cl/PEI self-assemblies with different ratios. The HEA16Cl was synthesized according to a procedure reported in the literature [31]. M6PEI was prepared from an adapted procedure based on a stepwise aldimine formation-reduction in methanol [40], using dodecyl aldehyde as the alkylating agent of PEI (800 Da) in a 6:1 ratio (Scheme 1). The ^{1}H NMR analysis, based on the ratio of integrals of -CH_2- signals from the polymer backbone and those of -CH_2- signal from the alkyl chain, confirmed the complete conversion of primary amines into secondary, thus providing a new polymer M6PEI with a 6:1 Dodecyl:PEI ratio. This method proved to be very straightforward in the selective alkylation of primary amines and could be applied for a variety of commercially available aldehydes.

- Scheme 1 –

In a first set of experiments, the formation of polymer-surfactant complexes was characterized in water. The steady state fluorescence spectroscopy was chosen as an alternative to surface tension experiments [27]. Pyrene is commonly used as a probe since its fluorescence emission spectrum is sensitive to the polarity of the medium [41, 42].

The *cmc* value of M6PEI and the *cac* value between M6PEI and HEA16Cl were extracted from the graphs in Figure 2a and 2b, respectively. While the commercial PEI does not exhibit hydrophobic domains and self-aggregation [27], we showed that the synthesized M6PEI bearing an average of six lipophilic alkyl chains with 12 carbon atoms self-aggregate into micelles above critical micellar concentrations (*cmc*) of 0,084 mmol L^{-1} in monomer units or 0.002 mmol L^{-1} using the average molecular weight determined by ^{1}H NMR. The aggregation behaviour of M6PEI and HEA16Cl was determined at 0.089 mmol L^{-1} that is 13.8 times lower than the *cmc* of HEA16Cl (1.23 mmol L^{-1}) [31]. For the *cac* determination the concentration of M6PEI was 0,058 mmol L^{-1} (monomer units), which is lower that its cmc. These investigations demonstrated that the mixed aggregation occurs as also previously observed by surface tension experiments of binary systems PEI and cationic surfactants in aqueous medium [43]. Moreover, the *cac* values of unmodified PEI and cationic surfactants are also in agreement with our work, being observed at 0.09 mmol L^{-1} of CTAB using a 0.5 mol L^{-1} of PEI while the *cmc* of CTAB alone is 0.8 mmol L^{-1} [43].

- Figure 2 –

The colloidal NPs were obtained by chemical reduction of Na_2PdCl_4 with sodium borohydride, in the presence of the appropriate stabilizing agent (HEA16Cl, M6PEI or HEA16Cl/M6PEI mixture). The palladium concentration was fixed at 1.50×10^{-2} mmol L^{-1}. Several mixtures have been investigated according to the MPEI:HEA ratio such as M6PEI:HEA16Cl = 1:4 (Mix1); M6PEI:HEA16Cl = 2.5:2.5 (Mix2); and M6PEI:HEA16Cl = 4:1 (Mix3). In a first approach, the suitable amount of stabilizing agent, ranging from 1 to 5 eq., was optimized, and the stability of the as-prepared Pd^{0}NPs suspensions were visually estimated to ensure that no sedimentation takes place. The stability was also evaluated after

the catalytic tests of hydrogenation of cyclooctene under atmospheric hydrogen pressure as model reaction (Scheme 2). The results are gathered in Table 1.

- Scheme 2 –

Among the various stabilizer/Pd ratios, the best catalytic results, in association with a good stability, were achieved with a ratio of 5, either for the ammonium salt HEA16Cl alone or for M6PEI-HEA16Cl mixture (Entries 3 and 7, respectively). In similar reaction conditions (room temperature, 1 bar H_2), the system stabilized with M6PEI alone provides a lower activity in the cyclooctene hydrogenation and a poor stability during catalysis. In the case of a polymer/surfactant self-assembly, best results were achieved with M6PEI/HEA16Cl ratio of 1:4 (Entry 7). The highest catalytic activity was achieved at lower concentrations of protective agent (Entry 1) but the colloidal dispersions are less stable, leading to a precipitate of Pd black during the reaction. The use of polymer alone (M6PEI) led to unstable NPs for the cyclooctene hydrogenation, but proved to be active and stable at higher pressure and for other substrates before and after catalysis, as discussed later.

- Table 1 -

2.2 Characterization of Pd^0NPs.

The shape, morphology and size distribution of the Pd^0NPs were determined through TEM, SAXS and DLS measurements. TEM micrographs (Figure 3a-e) showed that the stabilizers used in the NPs synthesis strongly influence the particles size and morphology. The Pd^0NPs capped with HEA16Cl were spherical with an average diameter of 1.8 ± 0.3 nm (Table 2). In contrast, worm-like structures, with sizes about 4.0 ± 1.8 nm, were observed with M6PEI as capping agents, which could be attributed to the morphology of M6PEI micelles formed in the aqueous medium. For the mixed systems, the average size is relative

to the HEA16Cl/M6PEI ratio used in the synthesis, with a tendency of larger sizes with an increase in M6PEI concentration. The Pd^0NPs sizes are resumed in Table 2.

- Figure 3 -

- Table 2 –

The Pd^0NPs were also analysed by Synchrotron based SAXS and a bench top set-up, and the data fitted to a Beaucage Power Law [37] and Core-Shell models [38]. As observed in the microscopy analysis, the presence of small agglomerates for all systems is evidenced in the SAXS spectra (Figure 3, f-j), which could be modelled with a mass fractal approach [44-46]. SAXS spectra showed two weak oscillations about 0.35 nm^{-1} and ± 1 nm^{-1} for M6PEI system, which could be correlated to different size domains, composed by core-shell organic/metal system, respectively (Figure 3g). In opposition to M6PEI, a significant bump was observed about ± 1.05 nm^{-1} due to the metallic core in the case of HEA-stabilized PdNPs (Figure 3f). The same bumps were present all samples (Figure 3h-j). In the case of Mix2 and Mix3 a Core-Shell model could be applied since the scattering contrast (SLD) between the solvent, organic layer and metallic core were different [47], the results were analogous to those obtained by the Beaucage Fitting. The unified exponential/power law introduced by Beaucage provided a smooth transition between Guinier and power-law (Porod) regimes in which different hierarchical levels can be measured quantitatively. Since both mathematical expressions could simulate the data with good agreement with TEM and DLS measurements, the results were used in this work.

Moreover, the difference between the micellar double-layer diameter and the metallic core size shows that the double layer composed by the surfactant HEA has a thickness of about 3 nm (Figure 4). According to their spatial organisation [31] and the bond length of the carbon chains in the HEA16Cl molecules (0.154 nm for C-C bonds and 0.149 nm for $C\text{-}N^+$ bonds), it could be stated that the HEA molecules are strained and have normal orientation

at the particle's surface, as illustrated in Figure 4. Finally, the organic shell in the systems based on M6PEI possesses a size around 4 to 5 nm, which is in good agreement with previous works on determination of shell thickness [48-50] considering the organic double-layer formed by the surfactants and the polymer molecules [31].

– Figure 4 –

From DLS analyses, the average hydrodynamic diameters (D_H), obtained from the correlation curves of the light scattering of each sample, fitted using the CONTIN algorithm, were determined to be 7.0 and 20.7 nm for HEA16Cl and M6PEI-stabilized Pd^0NPs, respectively. These values are strongly correlated with the SAXS experiments and also show the cooperative effect of both components in the stabilisation of Pd^0NP. In the case of HEA/ M6PEI mixtures, the increase in M6PEI amount has an influence on the D_H of the resulting colloids, with a size increase from 12 nm for Mix1 to 17.7 nm and 19.6 nm for Mix2 and Mix3, respectively (Table 2).

The good stability of the Pd^0NPs could be related to an efficient electrostatic stabilization, as confirmed by the zeta potential (ζ) values, given in Table 2. In all cases, the colloidal suspensions have a high positive apparent charge, ranging from +47 to +72 mV, thus allowing a significant electrostatic repulsion (Coulombic interactions) induced by the protective agents, which provides a good stabilisation of Pd^0NPs. Moreover, a pertinent linear correlation (R^2 = 0.964) was observed between the ζ-potential values and the amount of M6PEI in various systems (Figure 5), according to M6PEI/HEA16Cl ratio from 0 (pure M6PEI) to 100% (pure HEA). In fact, the increase of the ζ-potential values was correlated to the presence and amount of HEA. The relationship between the ζ-potential and the amount of co-stabilizer (either HEA or M6PEI) shows that both compounds have a positive influence in the stability, as well as in the catalytic activity of the suspension (Table 1). We can conclude that M6PEI and HEA act together as cooperative protective agents and the

increasing charge density upon adding a cationic surfactant to a weak positive polyelectrolyte is reflected in the obtained ζ-potential distributions.

Finally, the pH values measured for the colloidal dispersions were in agreement with the chemical composition of the stabilizers used, alone or mixed (Table 2). In fact, the pH values of the surfactant solutions have a tendency to be slightly acid, in opposition to those containing higher concentrations of M6PEI, which behaves as a positively charged weak polyelectrolyte in aqueous solution.

– Figure 5 –

2.3 Catalytic studies.

In the first set of catalytic experiments (Table 1), the Pd^0NPs stabilized with ammonium surfactant alone with a Pd/Stabilizer ratio of 5, afforded the best result in terms of stability in the cyclooctene hydrogenation with a specific activity (SA) about 80 h^{-1} (Table 1, Entry 3). The SA values were defined as mol of transformed substrate per mol of introduced Pd per hour [51] and were determined by kinetic follow-up of the reaction by extraction of small aliquots of the reaction medium over time (Figure 6). From physico-chemical characterizations, the HEA16Cl@Pd^0NPs suspension displays a smaller hydrodynamic diameter (D_H) and a higher ζ-potential value, than M6PEI or mixed systems as protective agents. These features could be responsible for an easier access of the substrate at the Pd^0NPs surface, resulting in a higher catalytic activity and stability. The stability of the suspensions was considered relating to the presence/absence of sedimentation particles by visual inspection of the aqueous dispersions. Based on the ζ-potential values, the results show that the presence of HEA16Cl additively increases the stability of the dispersion (Table 2).

- Figure 6 –

In the absence of HEA16Cl, a poor conversion (~ 6%) in cyclooctane was obtained with a pure polymer system (Table 1, Entry 5). However, an increase in the hydrogen

pressure (up to 2 bar of H_2) leads to a specific activity (SA) of 48.5 h^{-1} with 97% conversion in 2 h, which is two times the SA value observed by Neumann with similar colloidal alkylated PEI catalytic systems [24]. The kinetics increase could be due to a better solubilisation of the substrate [52] and/or a better adsorption of H_2 in the surface of the Pd^0NPs under pressure [53]. Finally, the M6PEI-stabilized Pd^0NPs did not show a good stability during a longer reaction time under mild conditions (room temperature, 1 bar of H_2) in opposition to the reaction performed at 2 bar of H_2 that offers a better stability and a complete conversion. Benefiting from the kinetics, the absence of sedimentation after the extraction of products by diethyl ether attests the better behaviour in this condition. Finally, an increase in the catalytic activity was observed according to the amount of HEA introduced within the mixture (Table 1, Entries 7-9). The SA values determined on the basis of an optimized time for a total conversion decreases in the following order: HEA > Mix1 > Mix2 > Mix3 > M6PEI. In the same manner as for the ζ-potential correlation with the surfactant/polymer ratio in the supramolecular self-assembly, the catalytic activity in hydrogenation reactions could be rationalized with the M6PEI/HEA ratios for cyclooctene **1** and 5-methyl-3-hexen-2-one **2**. Previously, Farin and Avnir have demonstrated a relation between the catalytic activity defined as mol $time^{-1}$ $particle^{-1}$ and the particle size of supported heterogeneous catalysts [54]. In this study, such a relation within the particle average size was not observed but the physico-chemical properties induced by the capping agents proved to be relevant parameters. Undoubtedly, a good correlation was demonstrated between the SA and the amount of HEA surfactant in the cyclooctene hydrogenation (Figure 7a). In the same manner, a good structure/activity relationship was also demonstrated during the hydrogenation of the internal C-C double bond of 5-methyl-3-hexen-2-one **2**, tested as a linear *α,β*-unsaturated ketone (Figure 7b).

– Figure 7 –

The catalytic performances of the palladium nanocatalysts developed in the present paper were compared with various Pd heterogeneous catalysts (Table 3), already reported in

the literature, considering the cyclooctene hydrogenation. The best result has been obtained with Pd@C12Im-PEG IL under 10 bar of H_2 [55]. Nevertheless, in absolute SA values, the present Pd(0) species demonstrated promising performances in terms of conversion among the best results at room temperature and mild H_2 pressure in water as a benign and environment-friendly reaction medium. No straightforward comparison with the different systems is possible due to the different variables employed in each study, only in the case of Neumann and coworkers [24] (Table 3, entry 4) and M6PEI (Table 3, entry 3) in which our work showed better results, possibly due to the different methodology of PEI modification and probably the polymer molecular weight (50 kDa versus 800 Da).

- Table 3 -

In a second set of experiments, both catalysts, capped either with HEA surfactant or M6PEI polymer, were investigated in a competitive reaction between two substrates, possessing different degrees of steric hindrance. Cyclooctene **1** and 1-octene **3** were chosen as substrates in a 1:1 ratio. As presented in Scheme 3 and Figure 8, the M6PEI@Pd^0NPs showed higher selectivity than the HEA system. The kinetics study (Figure 8a) displays that M6PEI@Pd^0NPs could selectively reduce the less hindered double bond in very good yields. The double layer formed by the polymer around the metal core might influence the geometrical arrangements and conformations of the substrates, as well as their mobility, when approaching the catalyst's surface, thus impacting the catalytic activity [56].

– Scheme 3 –

In contrast, both substrates were simultaneously reduced after 1.5 h, with quantitative conversion in 60 min for 1-octene and 90 min for cyclooctene with HEA@Pd^0NPs system (Figure 8b). The slight differences in the reaction rates could be explained by small differences in terms of water-solubility and steric hindrance of both substrates as well as to

the molecular structure of the polymer and the surfactant. Indeed, the branched M6PEI seems to be more sensitive to hindered double bonds as seen in Table 3 (entries 3 and 4) and in the competition reactions. Similar results have already been reported with dendrimers [25], with a decrease in catalytic activity and selectivity towards less hindered substrates when increasing the dendrimer generation.

– Figure 8 –

In a final step, the performances of the catalysts were also evaluated in the hydrogenation of various linear and cyclic *α,β*-unsaturated ketones (enones, Scheme 4), conducted in a pure biphasic water/substrate medium, under mild conditions (room temperature and 1 bar H_2). The results are gathered in Table 4. In all cases, the reaction was selective towards the C=C bonds, with no C=O reduction for both cyclic and acyclic substrates. The less hindered compounds **2**, **4** and **5** were totally converted into the respective ketones in quantitative yields in less than 1 hour (Entries 1-3). As reported with cyclooctene, the HEA@Pd^0NPs yielded the best results, with a specific activity up to 1176 h^{-1} (Entry 2).

– Scheme 4 –

In the same manner, even if high yields were achieved, lower activities were observed with pure M6PEI and particularly with cyclic enone **5** in comparison with acyclic enone **2**, showing the great influence of its polymeric backbone.

Both M6PEI/HEA mixtures (Mix1, Mix2) were investigated in the hydrogenation of enones, with complete conversions achieved under mild conditions and a higher activity value for the mixture containing a higher amount of HEA (Mix2). Indeed, the surfactant could act as a phase transfer agent [57], thus solubilising the lipophilic substrate, and also as a

protective agent in the dynamic supramolecular organization [58] around the particle, thus facilitating the access of the substrate onto the metallic surface.

In terms of stereo-control, the hydrogenation reaction of the prochiral isophorone **6** yielded a racemic hydrogenated product **6'** for all catalysts, as expected; however, no reaction was observed for M6PEI@Pd^0NPs. Moreover, the hindered substrate verbenone **7** was completely hydrogenated (97%) under higher pressure (10 bar H_2) in 2 h, using HEA@Pd^0NPs system (entry 5).

To summarize, the structure of *α,β*-unsaturated ketone seems to have an influence on the catalytic activity, as observed by Crooks and coworkers in the case of structurally related allylic alcohols [25]. Indeed, the highest specific activity was achieved for the conversion of **3** with HEA@Pd^0NPs. Moreover, the presence of a methyl group on the C=C bond strongly slows the reaction rate when comparing the data for **4** and **5**. The trend is also observed for the substrates **6** and **7**, shown by the lack of catalytic activity of M6PEI@Pd^0NPs.

– Table 4 –

To estimate the efficiency of our systems based on Pd nanoparticles, a comparison with Pd catalysts well described in the literature for the hydrogenation of cyclohexenone **4** was resumed in Table 5. Undoubtedly, few of systems have been reported using water as reaction medium (entries 1-3, 9) and our Pd systems (entries 1-3) were relevant with a good activity under atmospheric pressure. Moreover, M6PEI@Pd^0NPs (Table 5, Entry 3 and Mix1@PdNPs (Table 5, entry 2) provide better activity in aqueous medium (SA = 294 h^{-1} and 388 h^{-1} respectively) than the other catalysts from the literature. Finally, the best catalytic activity was reported by Zhang [59] with a value of 1176 h^{-1} which is similar to the best value obtained in this work. In comparison with others, the activity of the nanoparticles stabilised by polymers, surfactants and its mixtures and the reaction parameters represent an advance towards greener transformations.

– Table 5 –

3. Conclusions

The paper describes a novel preparation of PEI derivatives and its assemblies with a cationic surfactant, HEA16Cl, and their use as stabilizers for aqueous palladium nanoparticles. The supramolecular self-assemblies composed of a modified PEI and an ammonium surfactant (HEA16Cl) have been investigated as efficient protective agents of catalytic Pd^0NPs in hydrogenation reactions and compared with M6PEI or HEA salts alone as references. All catalytic systems were fully characterized by SAXS, TEM, as well as DLS experiments, leading to a good correlation of these different techniques to determine the particle size. These self-assemblies capped Pd^0NPs have been investigated in the hydrogenation of alkenes and several linear or cyclic *α,β*-unsaturated ketones in pure biphasic liquid-liquid water/substrate medium under mild conditions (1 bar H_2, rt). Although HEA@Pd^0NPs proved to be powerful in terms of kinetics, probably due to a dynamic behaviour of the protective layers facilitating the solubilisation of the substrate and its access onto the Pd surface, various mixtures of M6PEI/HEA proved also to be efficient in terms of stability and catalytic reactivity.

Acknowledgements

We are grateful to CNPq and CAPES for financial support received for this study under the Science Without Borders Program (SWE 200723/2014-6). This work was also supported by the Brazilian Synchrotron Light Laboratory (LNLS) under proposal SAXS1-15973 (beam time usage) and the Central Laboratory of Electron Microscopy (LCME) at UFSC (TEM analysis). The authors are indebted to Patricia Beaunier from Université Pierre et Marie Curie (UMPC) for transmission electron microscopy analysis and Franck Artzner from Institut de Physique at Université de Rennes for additional SAXS analysis and discussions.

Bibliographic References

[1] J. Grunes, J. Zhu, G.A. Somorjai, Chem. Commun., (2003) 2257.

[2] N. Yan, C. Xiao, Y. Kou, Coord. Chem. Rev., 254 (2010) 1179-1218.

[3] R. Jin, Nanotechnol. Rev., 1 (2012) 31-56.

[4] V. Polshettiwar, T. Asefa, Nanocatalysis : synthesis and applications, John Wiley & Sons, Inc., Hoboken, New Jersey, 2013.

[5] K. An, G.A. Somorjai, ChemCatChem, 4 (2012) 1512-1524.

[6] E. Roduner, Chem. Soc. Rev., 35 (2006) 583.

[7] F. Zaera, ChemSusChem, 6 (2013) 1797-1820.

[8] H. Lee, RSC Adv., 4 (2014) 41017-41027.

[9] P. Serp, K. Philippot, G.A. Somorjai, B. Chaudret, Nanomaterials in Catalysis, Wiley VCH, Weinheim, Germany, 2012.

[10] E.-i. Negishi, Handbook of Organopalladium Chemistry for Organic Synthesis, John Wiley & Sons, Inc., Hoboken, New Jersey, 2002, 2716.

[11] L.A. Saudan, Acc. Chem. Res., 40 (2007) 1309-1319.

[12] I. Favier, D. Madec, E. Teuma, M. Gomez, Curr. Org. Chem., 15 (2011) 3127-3174.

[13] A. Balanta, C. Godard, C. Claver, Chem. Soc. Rev., 40 (2011) 4973.

[14] D.J. Gavia, Y.-S. Shon, ChemCatChem, 7 (2015) 892-900.

[15] M. Moreno-Mañas, R. Pleixats, Acc. Chem. Res., 36 (2003) 638-643.

[16] I.P. Beletskaya, L.M. Kustov, Russ. Chem. Rev., 79 (2010) 441-461.

[17] D. Prat, A. Wells, J. Hayler, H. Sneddon, C.R. McElroy, S. Abou-Shehada, P.J. Dunn, Green Chem., (2015).

[18] D. Prat, O. Pardigon, H.-W. Flemming, S. Letestu, V. Ducandas, P. Isnard, E. Guntrum, T. Senac, S. Ruisseau, P. Cruciani, P. Hosek, Org. Process Res. Dev., 17 (2013) 1517-1525.

[19] V. Polshettiwar, R.S. Varma, Green Chem., 12 (2010) 743.

[20] R. Breslow, The Principles of and Reasons for Using Water as a Solvent for Green Chemistry, into: Handbook of Green Chemistry, Wiley-VCH Verlag GmbH & Co. KGaA, 2010.

[21] I. Beletskaya, V. Tyurin, Molecules, 15 (2010) 4792-4814.

[22] Z. Niu, Y. Li, Chem. Mater., 26 (2014) 72-83.

[23] R.-Y. Zhong, K.-Q. Sun, Y.-C. Hong, B.-Q. Xu, ACS Catal., 4 (2014) 3982-3993.

[24] M.V. Vasylyev, G. Maayan, Y. Hovav, A. Haimov, R. Neumann, Org. Lett., 8 (2006) 5445-5448.

[25] Y. Niu, L.K. Yeung, R.M. Crooks, J. Am. Chem. Soc., 123 (2001) 6840-6846.

[26] M. Abe, J.F. Scamehorn, Mixed surfactant systems, 2nd ed., Marcel Dekker, New York, 2005.

[27] I.C. Bellettini, L.G. Nandi, R. Eising, J.B. Domingos, V.G. Machado, E. Minatti, J. Colloid Interface Sci., 370 (2012) 94-101.

[28] A.C. Felippe, I.C. Bellettini, R. Eising, E. Minatti, F.C. Giacomelli, J. Brazil. Chem. Soc., 22 (2011) 1539-1548.

[29] I.C. Bellettini, R. Eising, A.C. Felippe, J.B. Domingos, E. Minatti, V.G. Machado, Quim. Nova, (2015).

[30] G.M. Whitesides, M. Boncheva, PNAS, 99 (2002) 4769-4774.

[31] E.G. Bile, R. Sassine, A. Denicourt-Nowicki, F. Launay, A. Roucoux, Dalton Trans., 40 (2011) 6524-6531.

[32] W.C. Elias, R. Eising, T.R. Silva, B.L. Albuquerque, E. Martendal, L. Meier, J.B. Domingos, J. Phys. Chem. C, 118 (2014) 12962-12971.

[33] K.O. Santos, W.C. Elias, A.M. Signori, F.C. Giacomelli, H. Yang, J.B. Domingos, J. Phys. Chem. C, 116 (2012) 4594-4604.

[34] A.M. Signori, K.O. Santos, R. Eising, B.L. Albuquerque, F.C. Giacomelli, J.B. Domingos, Langmuir, 26 (2010) 17772-17779.

[35] L.P. Cavalcanti, I.L. Torriani, T.S. Plivelic, C.L.P. Oliveira, G. Kellermann, R. Neuenschwander, Rev. Sci. Instrum., 75 (2004) 4541-4546.

[36] A.P. Hammersley, Scientific software FIT2D, in, http://www.esrf.eu/computing/scientific/FIT2D, 2009.

[37] G. Beaucage, J. Appl. Crystallogr., 29 (1996) 134-146.

[38] A. Guinier, G. Fournet, Small-angle scattering of X-rays, Wiley, New York, 1955.

[39] J. Kohlbrecher, Software package SASfit for fitting small-angle scattering curves, in, http://kur.web.psi.ch/sans1/SANSSoft/sasfit.html, 2009.

[40] A.F. Abdel-Magid, K.G. Carson, B.D. Harris, C.A. Maryanoff, R.D. Shah, J. Org. Chem., 61 (1996) 3849-3862.

[41] F.M. Winnik, S.T.A. Regismond, Colloids And Surfaces A, 118 (1996) 1-39.

[42] E.D. Goddard, N.J. Turro, P.L. Kuo, K.P. Ananthapadmanabhan, Langmuir, 1 (1985) 352-355.

[43] L.Y. Zakharova, A.B. Mirgorodskaya, E.I. Yackevich, A.V. Yurina, V.V. Syakaev, S.K. Latypov, A.I. Konovalov, J. Chem. Eng. Data, 55 (2010) 5848-5855.

[44] J.M. Lin, T.L. Lin, U.S. Jeng, Y.J. Zhong, C.T. Yeh, T.Y. Chen, J. Appl. Crystallogr., 40 (2007) S540-S543.

[45] M. Singh, I. Sinha, A.K. Singh, R.K. Mandal, J. Nanopart. Res., 13 (2010) 69-76.

[46] D. Aili, P. Gryko, B. Sepulveda, J.A.G. Dick, N. Kirby, R. Heenan, L. Baltzer, B. Liedberg, M.P. Ryan, M.M. Stevens, Nano Lett., 11 (2011) 5564-5573.

[47] J.P. Patterson, M.P. Robin, C. Chassenieux, O. Colombani, R.K. O'Reilly, Chem. Soc. Rev., 43 (2014) 2412.

[48] B.T. Diroll, K.M. Weigandt, D. Jishkariani, M. Cargnello, R.J. Murphy, L.A. Hough, C.B. Murray, B. Donnio, Nano Lett., 15 (2015) 8008-8012.

[49] S. Kerkhofs, T. Willhammar, H. Van Den Noortgate, C.E.A. Kirschhock, E. Breynaert, G. Van Tendeloo, S. Bals, J.A. Martens, Chem. Mater., 27 (2015) 5161-5169.

[50] T. Schindler, M. Schmiele, T. Schmutzler, T. Kassar, D. Segets, W. Peukert, A. Radulescu, A. Kriele, R. Gilles, T. Unruh, Langmuir, 31 (2015) 10130-10136.

[51] C. Evangelisti, N. Panziera, A. D'Alessio, L. Bertinetti, M. Botavina, G. Vitulli, J. Catal., 272 (2010) 246-252.

[52] A. Bouriazos, S. Sotiriou, P. Stathis, G. Papadogianakis, Appl. Catal. B-Environ., 150-151 (2014) 345-353.

[53] G.S. Fonseca, J.B. Domingos, F. Nome, J. Dupont, J. Mol. Catal. A-Chem, 248 (2006) 10-16.

[54] D. Farin, D. Avnir, J. Am. Chem. Soc., 110 (1988) 2039-2045.

[55] W. Zhu, H. Yang, Y. Yu, L. Hua, H. Li, B. Feng, Z. Hou, Phys. Chem. Chem. Phys., 13 (2011) 13492.

[56] A.B.R. Mayer, Polym. Advan. Technol., 12 (2001) 96-106.

[57] C.M. Starks, ACS Sym. Ser., 326 (1987) 1-7.

[58] R. Zana, Dynamics of surfactant self-assemblies : micelles, microemulsions, vesicles, and lyotropic phases, Taylor & Francis/CRC Press, Boca Raton, 2005, p. 1-25.

[59] Y. Zhang, X.-Y. Quek, L. Wu, Y. Guan, E.J. Hensen, J. Mol. Catal. A-Chem, 379 (2013) 53-58.

[60] Q.M. Kainz, R. Linhardt, R.N. Grass, G. Vilé, J. Pérez-Ramírez, W.J. Stark, O. Reiser, Adv. Funct. Mater., 24 (2014) 2020-2027.

[61] U.R. Pillai, E. Sahle-Demessie, J. Mol. Cat. A-Chem , 222 (2004) 153-158.

[62] L. Wang, S. Shylesh, D. Dehe, T. Philippi, G. Dörr, A. Seifert, Z. Zhou, M. Hartmann, R.N. Klupp Taylor, M. Jia, S. Ernst, W.R. Thiel, ChemCatchem, 4 (2012) 395-400.

[63] Y. Hu, H. Yang, Y. Zhang, Z. Hou, X. Wang, Y. Qiao, H. Li, B. Feng, Q. Huang, Catal Commun.,10 (2009) 1903-1907.

[64] M.L. Kantam, R. Kishore, J. Yadav, M. Sudhakar, A. Venugopal, Adv. Synth. Catal., 354 (2012) 663-669.

[65] L. Wu, Z.-W. Li, F. Zhang, Y.-M. He, Q.-H. Fan, Adv. Synth. Catal., 350 (2008) 846-862.

[66] A. Datta, M. Agarwal, S. Dasgupta, Catal. Surv. Asia, 8 (2004) 171-178.

[67] S. Ganji, S. Mutyala, C.K.P. Neeli, K.S.R. Rao, D.R. Burri, RSC Adv., 3 (2013) 11533.

[68] Y.-W. Kim, M.-J. Kim, B Korean Chem. Soc., 31 (2010) 1368-1370.

Figures, schemes and tables captions

Figure 1. Representative illustration of the work based on various amphiphilic molecules (used alone or combined) as protective agents of the Pd core.

Scheme 1. Synthesis of M6PEI by reductive alkylation in MeOH/THF.

Figure 2. Pyrene steady-state fluorescence determination of (a) M6PEI *cmc* and (b) M6PEI/HEA16Cl *cac*. The connecting black lines can be used as a guide for the eyes and the red dashed line represents the *cmc* and *cac* points, respectively.

Scheme 2. Hydrogenation of cyclooctene **1** to cyclooctane **1'** catalysed by Pd^0NPs.

Table 1. Optimization of Stabilizer/Pd ratio by catalytic hydrogenation of cyclooctene **1**[a].

Figure 3. TEM images and SAXS analysis for HEA (a, f), M6PEI (b, g), Mix1(c, h), Mix2 (d, i) and Mix3 (e, j).

Table 2. Physico-chemical characterizations of Pd^0NPs capped with various protective agents.

Figure 4. Model organisation describing the size domains of Pd^0NP and stabilizers (a) HEA, (b) M6PEI, (c) Mix1 = M6PEI+HEA16Cl 1:4, Mix2 = M6PEI+HEA16Cl 2.5:2.5 and Mix3 = M6PEI+HEA16Cl 4:1.

Figure 5. Correlation of the Zeta-potential values and the amount of HEA used for the synthesis of Pd^0NPs, Mix1 = M6PEI+HEA16Cl 1:4, Mix2 = M6PEI+HEA16Cl 2.5:2.5 and Mix3 = M6PEI+HEA16Cl 4:1.

Figure 6. Kinetic profile for cyclooctene hydrogenation catalyzed by HEA16Cl@Pd^0NP, the specific activity (SA) was calculated when no significant changes in product formation occurs i.e. at 1.25 h. The dashed line can be used as a guide for the eyes.

Figure 7. Correlation of specific activity (SA) for hydrogenation of substrates (a) cyclooctene **1** and (b) 5-methyl-3-hexen-2-one **2** and amount of HEA in the mixtures used to prepare the Pd(0) colloids. Mix1 = M6PEI+HEA16Cl 1:4, Mix2 = M6PEI+HEA16Cl 2.5:2.5 and Mix3 = M6PEI+HEA16Cl 4:1..

Table 3. Activities of different catalysts in the hydrogenation of cyclooctene catalysed by palladium species.

Scheme 3. Hydrogenation reaction competition of cyclooctene **1** and 1-octene **3** catalysed by palladium nanocatalysts.

Figure 8. Kinetic profiles for the competition hydrogenation reaction between 1-octene and cyclooctene catalysed by (a) M6PEI- and (b) HEA-capped Pd^0NPs. The dashed line can be used as a guide for the eyes.

Scheme 4. Hydrogenation of acyclic/cyclic enones **2**, **4** - **6** catalysed by palladium nanocatalysts.

Table 4. Catalytic hydrogenation of various linear and cyclic *α,β*-unsaturated ketones by Pd^0NPs.[a]

Table 5. Comparison of catalytic hydrogenation of cyclohexenone catalyzed by palladium catalysts.

Figure 1.

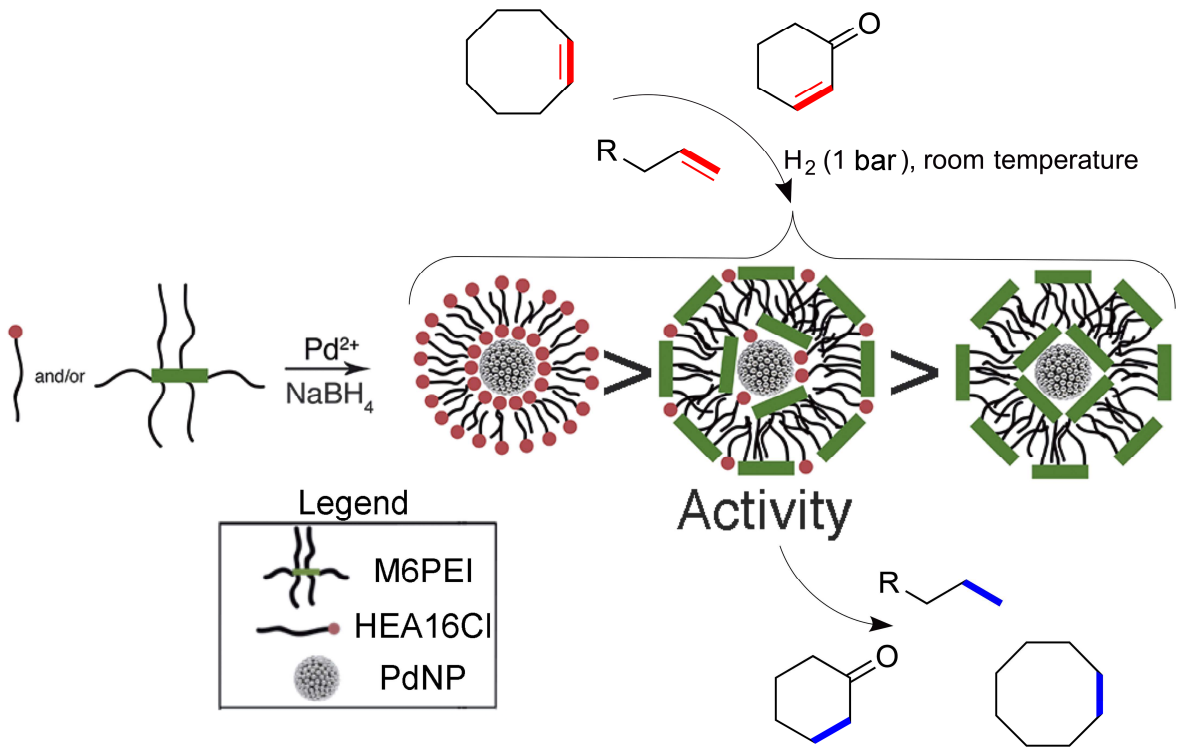
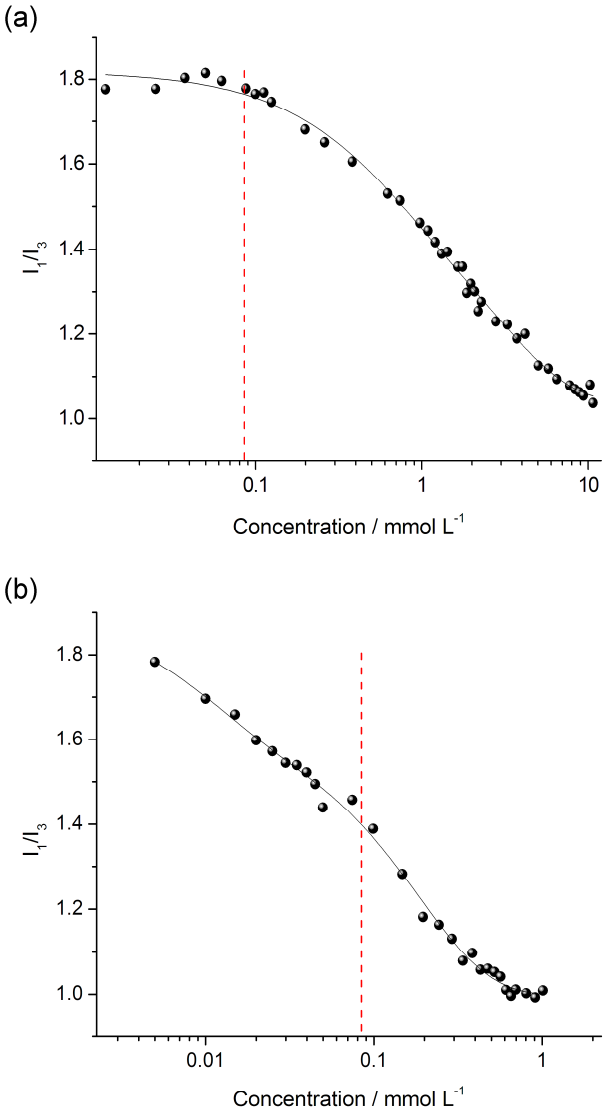
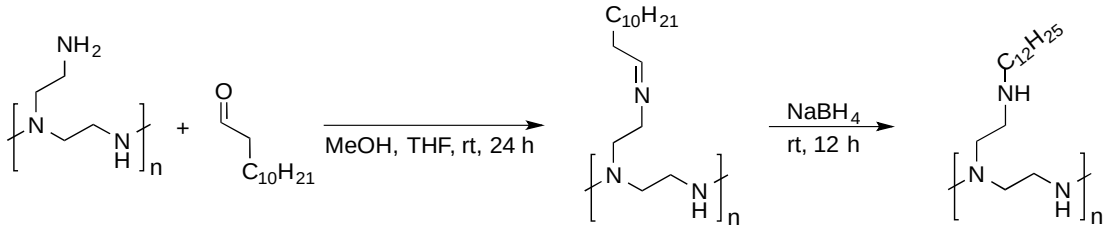

O
R
H2 (1 bar), room temperature
and/or
Pd2+
NaBH4
Activity
Legend
M6PEI
HEA16Cl
PdNP
R
O

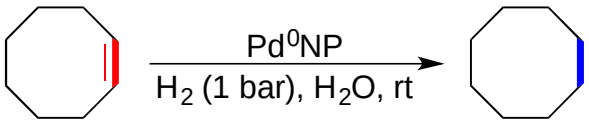
Figure 2.



Scheme 1.


NH2
N
N
H
n
+
O
C10H21
MeOH, THF, rt, 24 h
C10H21
N
N
N
H
n
NaBH4
rt, 12 h
C12H25
NH
N
N
H
n

Scheme 2.



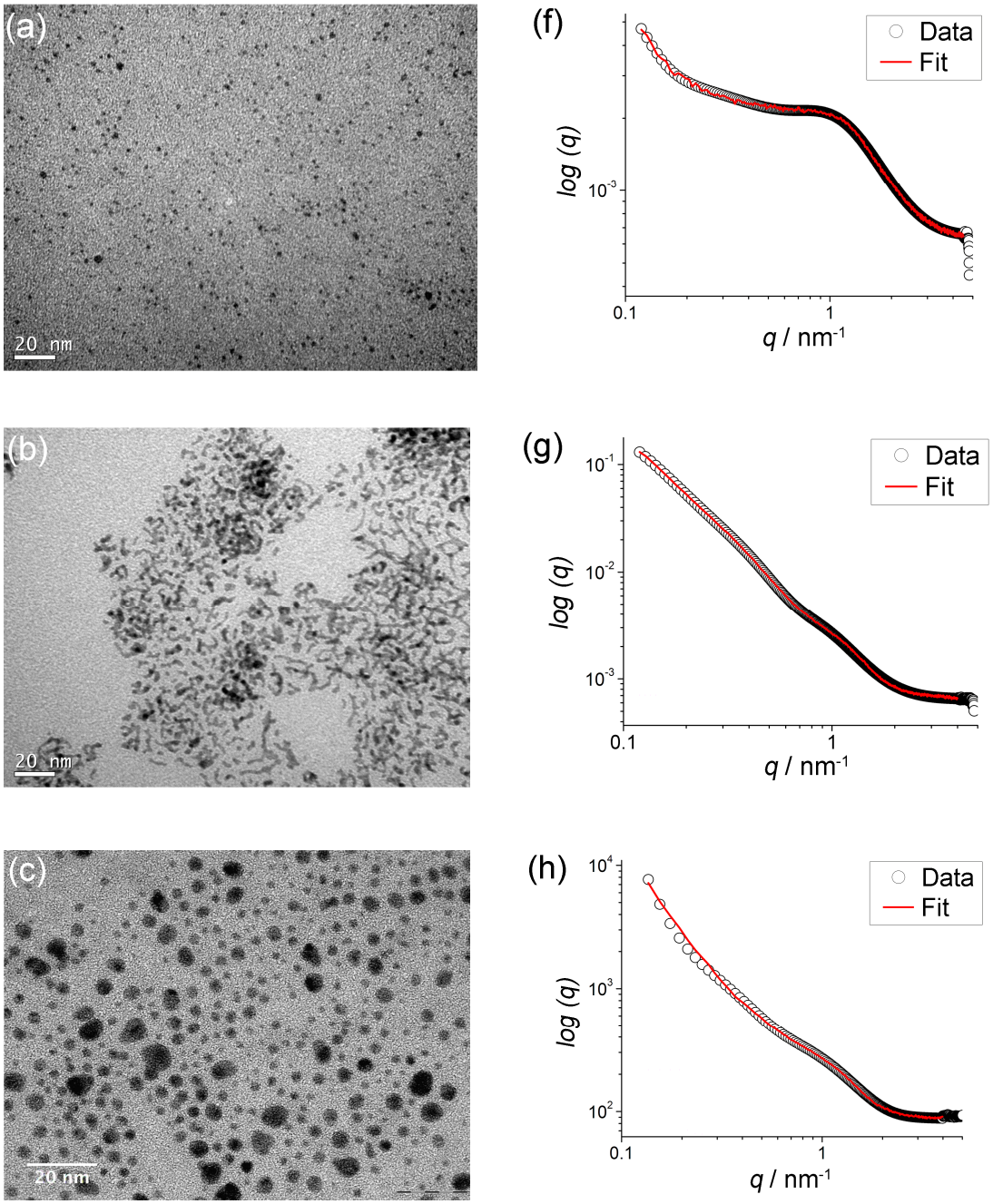
1 **1'**

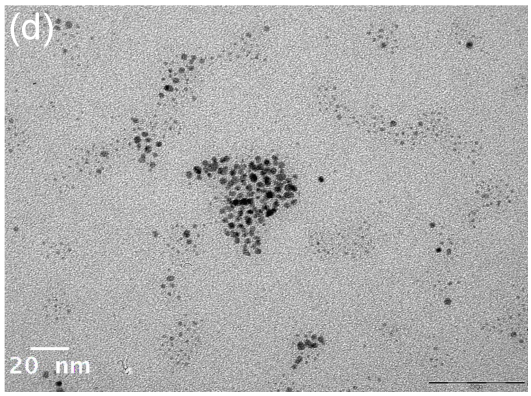
Table 1.

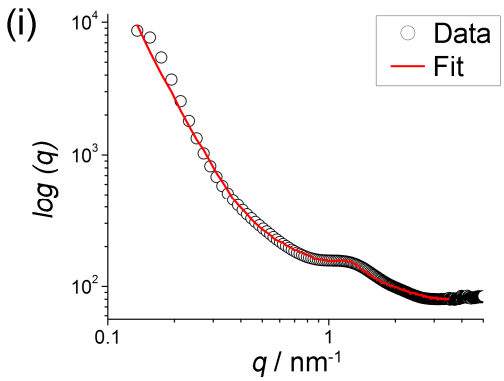
Entry	Stabilizer	Abbrev.	[Stabilizer]/[Pd] Ratio	[M6PEI]/[HEA16Cl] Ratio	Time (min)	Conversion (%)[b]	Specific Activity (h^{-1})[c]	Stability before catalysis	Stability after catalysis
1	HEA16Cl	HEA	1	-	30	100	200.0	yes	no
2	HEA16Cl	HEA	2	-	75	100	80.0	yes	no
3	HEA16Cl	HEA	5	-	75	96.8	77.6	yes	yes
4	M6PEI	M6PEI	2	-	45	61	81.3	yes	no
5	M6PEI	M6PEI	5	-	60	6[d]	6.0	yes	no[d]
6	M6PEI+HEA16Cl	Mix0	2	1:1	60	9.4	9.4	yes	no
7	M6PEI+HEA16Cl	Mix1	5	1:4	120	100	50.0	yes	yes
8	M6PEI+HEA16Cl	Mix2	5	2.5:2.5	300	95	25.0	yes	yes
9	M6PEI+HEA16Cl	Mix3	5	4:1	480	100	12.5	yes	yes

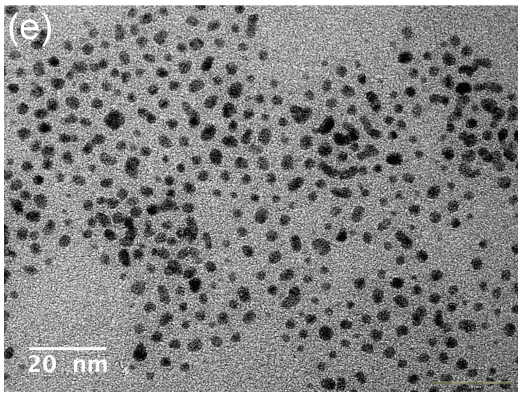
[a] Reaction conditions: Palladium (1.50×10^{-2} mmol), Cyclooctene/Metal molar ratio = 100, 1 bar H_2, rt, 10 mL H_2O. [b] Determined by GC analysis. [c] Specific Activity (SA) was defined as mol of transformed substrate /(mol of introduced Pd x h). [d] Stability after catalysis and 97% conversion was obtained after 2 hours under 2 bar of H_2 at room temperature.

Figure 3.


(a)
20 nm
(b)
20 nm
(c)
20 nm
(f)
Data
Fit
log (q)
10-3
0.1
1
q / nm-1
(g)
Data
Fit
log (q)
10-1
10-2
10-3
0.1
1
q / nm-1
(h)
Data
Fit
log (q)
10-4
10-3
10-2
0.1
1
q / nm-1







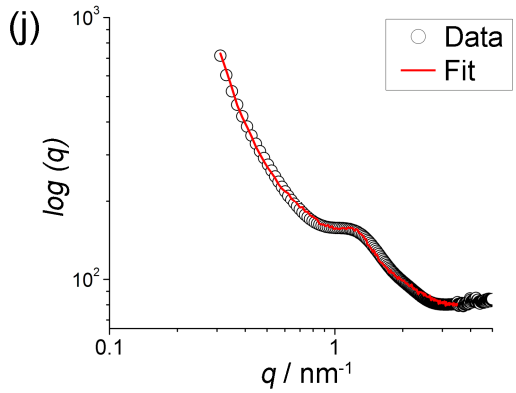


Table 2.

System	TEM (nm)	SAXS (nm)		D_H (nm)	ζ-Potential (mV)	pH
		Core	Core+Shell			
HEA	1.8 ± 0.3	1.75[a]	7.79[a]	7.0	+71.7	5.6
Mix1[c]	3.4 ± 1.1	3.98[a]	14.08[a]	12.0	+68.5	5.6
Mix2[d]	2.9 ± 1.0	2.88[b]	13.36[b]	17.7	+62.3	8.2
Mix3[e]	3.0 ± 1.0	2.90[b]	13.38[b]	19.6	+49.8	8.2
M6PEI	4.0 ± 1.8	4.85[a]	12.54[a]	20.7	+46.9	9.1

[a] Beaucage model. [b] Core-shell model. [c] Mix1 = M6PEI+HEA16Cl 1:4. [d] Mix2 = M6PEI+HEA16Cl 2.5:2.5. [e] Mix3 = M6PEI+HEA16Cl = 4:1.

Figure 4.

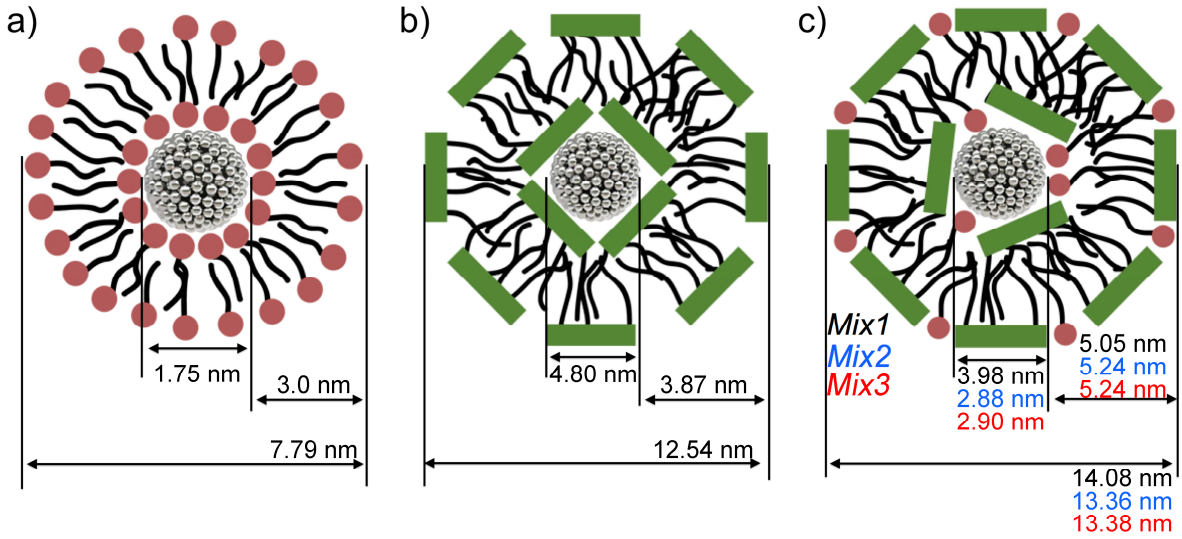

a)
1.75 nm
3.0 nm
7.79 nm
b)
4.80 nm
3.87 nm
12.54 nm
c)
Mix1
Mix2
Mix3
3.98 nm
2.88 nm
2.90 nm
5.05 nm
5.24 nm
5.24 nm
14.08 nm
13.36 nm
13.38 nm

Figure 5.

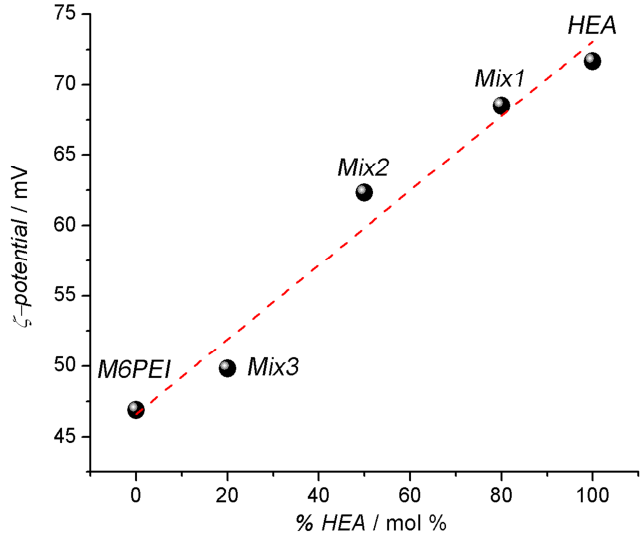

75
70
65
60
55
50
45
ζ-potential / mV
0
20
40
60
80
100
% HEA / mol %
HEA
Mix1
Mix2
Mix3
M6PEI

Figure 6.

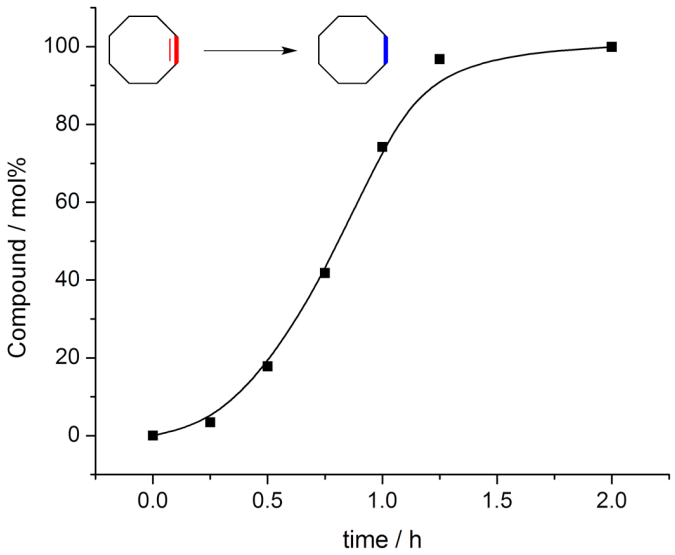


Figure 7.

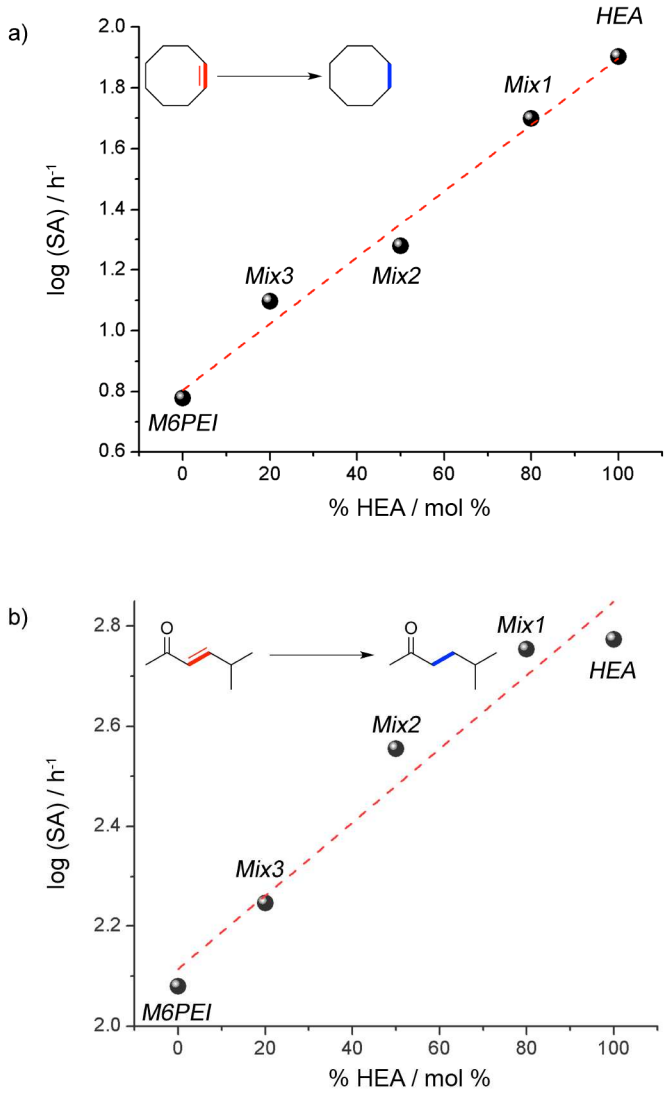
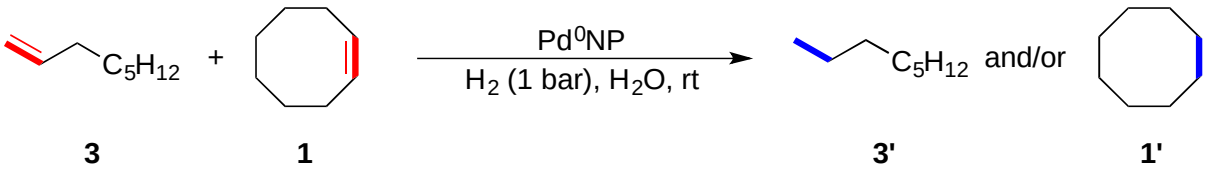

a)
HEA
Mix1
Mix3
Mix2
M6PEI
log (SA) / h-1
% HEA / mol %
b)
Mix1
HEA
Mix2
Mix3
M6PEI
log (SA) / h-1
% HEA / mol %

Table 3.

Entry	Catalyst	Ratio olefin/Pd	Solvent	Temp. (ºC)	H_2 Pressure (bar)	Time (h)	Conversion (%)	SA (h^{-1})
1	HEA[a]	100	H_2O	rt	1.0	1.25	100	77.6
2	Mix1[a]	100	H_2O	rt	1.0	2.0	100	50.0
3	M6PEI[a]	100	H_2O	rt	2.0	2.0	97	48.6
4	Pd@Alk-PEI[24]	122	H_2O	80	2.0	5.0	100	24.4
5	Pd@C12Im-PEG IL[55]	10000	H_2O	rt	10.0	3.0	100	6800
6	Pd@Co/C[60]	5000	i-PrOH	rt	1.0	4.0	100	1250.0
7	Pd@phen[61]	450	PEG400	50	1.0	8.0	100	56.3
8	Pd-Im@SiO_2[62]	6.7	Toluene	rt	1.0	48.0	64	0.1

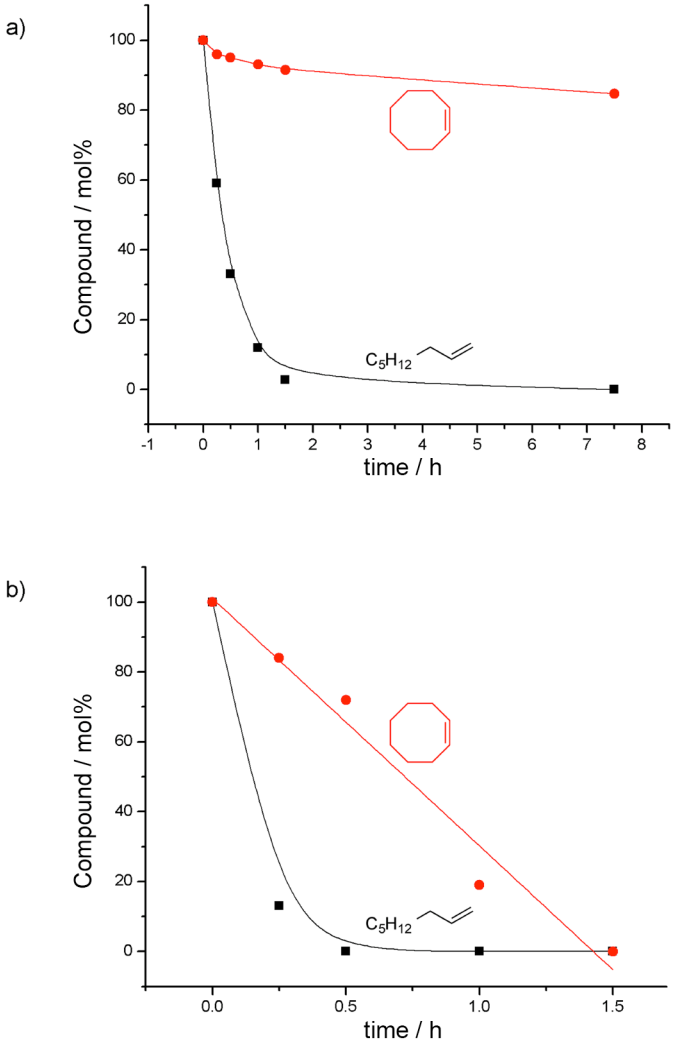
[a] This work.

Scheme 3.

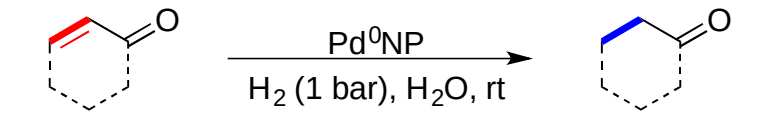


3 **1** **3'** **1'**

Figure 8



Scheme 4.



acyclic or cyclic
2, 4 - 6

acyclic or cyclic
2', 4' - 6'

Table 4.

Entry	Substrate	Product	M6PEI		HEA		Mix1		Mix2	
			Conv.[b] (%)	SA[c] (h^{-1})	Conv.[b] (%)	SA[c] (h^{-1})	Conv.[b] (%)	SA[c] (h^{-1})	Conv.[b] (%)	SA[c] (h^{-1})
1	5-methyl-hex-3-en-2-one (**2**)	5-methylhexanone (**2'**)	90	120	99	593	90	360	99	567
2	Cyclohexenone (**4**)	Cyclohexanone (**4'**)	100	294	98	1176	97	388	100	400
3	3-methyl-cyclohex-2-en-1-one (**5**)	3-methylcyclohexanone (**5'**)	100	23	100	200	96	192	100	200
4	Isophorone (**6**)[d]	3,3,5-Trimethylcyclohexanone (**6'**)	0	0	90	44.8	95	21	95	47.6
5	Verbenone (**7**)[e]	Verbanone (**7'**)[f]	0	0	0[g]	0[g]	0	0	0	0

[a] Reaction conditions: Palladium (1.50×10^{-2} mmol), Substrate/Metal molar ratio = 100/1, 1 bar H_2, rt, 10 mL H_2O. [b] Determined by GC analysis. [c] Specific Activity (SA) was defined as mol of transformed substrate /(mol of introduced Pd x h). [d] 3,3,5-Trimethyl-2-cyclohexen-1-one. [e] (1S,5S)-4,6,6-Trimethylbicyclo[3.1.1]hept-3-en-2-one and [f] (1S,4S,5S)-4,6,6-Trimethylbicyclo[3.1.1]heptan-2-one. [g] 97%, SA = 48.5 h^{-1} under 10 bar of H_2.

Table 5.

Entry	Catalyst	Ratio olefin/Pd	Solvent	Temp. (ºC)	H_2 Pressure (bar)	Time (h)	Conversion (%)	SA (h^{-1})
1	HEA[a]	100	H_2O	rt	1.0	0.08	98	1176
2	Mix1[a]	100	H_2O	rt	1.0	0.25	97	388
3	M6PEI[a]	100	H_2O	rt	1.0	0.33	98	294
4	Pd@phen[61]	450	PEG	40	1.0	8.0	100	52.8
5	Pd(10%)/PIL-Br[59]	400	MeOH	rt	10.0	0.33	89	1176
6	Pd-1[63]	1000	[BMMIM][PF_6]	rt	2.0	3.0	100	333
7	Pd/Mg-La[64]	1500	EtOH	rt	1.0	1.0	94	1410
9	G_2DenP-Pd[65]	200	1,4-Dioxane	60	15	8.0	95	23.5
11	Pd_{aq}[66]	100	THF	rt	1.0	1.0	98	98.0
12	5PdNPs-SBA-15[67]	100	H_2O	rt	1.0	2.0	100	50.0
13	Pd/Fe_3O_4[68]	333	MeOH	rt	1.0	0.5	97	646.0

[a] This work.